Infrared Study of Molecular Aggregation in the Poly(α-benzyl L-glutamate)/Benzyl Alcohol System

D. A. Prystupa and A. M. Donald*

Cavendish Laboratory, Madingley Road, Cambridge CB3 0HE, United Kingdom

Received June 2, 1992; Revised Manuscript Received October 26, 1992

ABSTRACT: Aggregation in poly(α-benzyl L-glutamate)/benzyl alcohol (PBLG/BA) systems has been studied by infrared spectroscopy. The amide and ester bands are found to be sensitive indicators of the state of aggregation. PBLG/BA gels are shown to consist of side by side aggregates of PBLG which melt in three stages. Side-chain motions commence near 40 °C (I) followed by fragmentation of polymer bundles into elementary fibrils (II) and dissociation of these elementary fibrils into individual polymer chains (III). Transition temperatures for stages II and III are dependent upon molecular weight. Transition III may be accompanied by subtle conformational changes in the α-helical molecular structure. Models of these conformational changes are proposed.

Introduction

Poly(α-benzyl L-glutamate) (PBLG) was first synthesized by Courtalds in the early 1950s as a potential silk replacement. This polypeptide has the chemical structure

$$R(CHC(=O)NH)_n$$

where R = $(CH_2)_2CO_2CH_2C_6H_5$.

The amide chain is common to all proteins and polypeptides. Different chemical species are distinguished by the R group(s). Although PBLG was not commercially suitable, PBLG has served as a model system for understanding the behavior of more complex polypeptide and, by extension, protein systems. The bewildering variety of phenomena exhibited by this relatively simple model polypeptide has stimulated research for four decades. Below, we outline those elements of a large body of literature accumulated over four decades which are germane to the present work.

The first spectroscopic studies of PBLG[1] provided evidence for a folded chain conformation which was shown shortly thereafter by X-ray diffraction[2] to correspond to the α-helical structure proposed by Pauling and Corey.[3] Subsequent infrared investigations[4-7] focused on elucidating relationships between spectra and the secondary structure. In the early 1970s, attention turned to Raman spectroscopy[8-11] with the advent of commercially available lasers. Recently, vibrational circular dichroism in the amide I region[12] and Raman spectra of the lattice region at low temperatures[13] have been reported. With one exception, the studies cited above used solid PBLG, typically deposited from dioxane or chloroform. These studies established that PBLG can assume four possible conformations: α-helical, extended β, cross β, or random coil. In the α-helical form, hydrogen bonds connect each residue with another, 3 units (13 atoms), along the same chain, forming a helix which completes 5 turns every 18 units. The intramolecular hydrogen bonds confer a degree of rigidity to the helical core of PBLG molecules so that the core behaves like a rigid rod. In the extended β form, the amide backbone of each molecule forms a planar zigzag in the direction of the fiber axis. Each amide group is hydrogen-bonded to an adjacent PBLG molecule lying in the same plane. The cross β form is similar to the extended β form except that the chains are perpendicular (rather than parallel) to the fiber axis. In all cases above, the monomers interact with one another via hydrogen bonding involving the hydrogen atom attached to the nitrogen atom and the carbonyl oxygen on the peptide group. Vibrational modes (amide bands) involving motions of these atoms are sensitive to the conformation. The observed amide frequencies vary between conformations depending upon the strength of hydrogen bonding and the magnitude of transition dipole moment coupling present in each conformation. The strength and ordering of hydrogen bonds, which are the main determinants of the conformation adopted, depend upon the molecular weight of the polypeptide, the solvent used, and the chirality of monomer units. Transition dipole moment coupling (TDC) was invoked by Krimm and Abe[14] to explain splittings of ca. 60 cm^{-1} observed between amide I components of polypeptides in the β conformations. TDC interactions are less significant for the α-helical conformation: splittings of ca. 4 cm^{-1} are expected.[15] Frequencies of selected vibrational bands as a function of conformation are given in Table I.

In this study, we shall focus attention on the amide I band and the ester band to probe the core and side chain of PBLG, respectively. Neither band seriously overlaps bands attributed to the solvent, benzyl alcohol (BA). Both bands are predominantly C=O stretching. The amide I band is modified by hydrogen bonding and dipole coupling interactions in the α-helical conformation, reducing the frequency by about 80 cm^{-1} compared to the unbound ester frequency. In the limiting case of a helix or infinite length, vibrational modes split into the following irreducible representation.[16]

$$\Gamma = A + B + E_1 + E_2 + E_3 + E_4 + E_5 + E_6 + E_7 + E_8$$

Optically active modes obey the $k = 0$ selection rule. The A and E_1 modes are infrared active and correspond to modes of vibration parallel (A) and perpendicular (E_1) to the molecular axis. The A, E_1, and E_2 modes are predicted to be Raman active. The remainder of the vibrational modes are optically inactive but contribute to the thermodynamic properties of the helix and may be observed by neutron scattering (for which no selection rules apply). In an oriented film, the parallel and perpendicular amide I bands lie at 1652 and 1655 cm^{-1}, respectively.[6] The same symmetry analysis is probably not applicable to the ester band. Previous studies[17] have reported side-chain packing with a periodicity different from the helical core in the solid. The parallel and perpendicular ester frequencies are 1734 and 1733 cm^{-1}, respectively.[6]

In the α-helical form, PBLG is a rodlike molecule with a propensity to form lyotropic liquid crystalline phases in a variety of solvents. The phase diagram of PBLG in

0024-9297/93/2226-1947$04.00/0

Table I
Conformationally Sensitive PBLG Frequencies (cm^{-1})

	α-helix[6]	β-sheet[7]	random coil[58]
C=O ester	1735 (π)[a]	1736	
	1733 (σ)[b]		
amide I	1652 (π)	1704 (0,π)	1660[c]
	1655 (σ)	1629 (π,0)	
amide II	1518 (π)	1524	1535
	1549 (σ)		
amide III	1328 (π)		
	1314 (σ)		
amide V		ca. 700	650
	613 (σ)		

[a] π, parallel band. [b] s, perpendicular band. [c] The traces shown in other papers[6,48] suggest that a better value for the amide I band in the random coil conformation would be between 1665 and 1670 cm^{-1}.

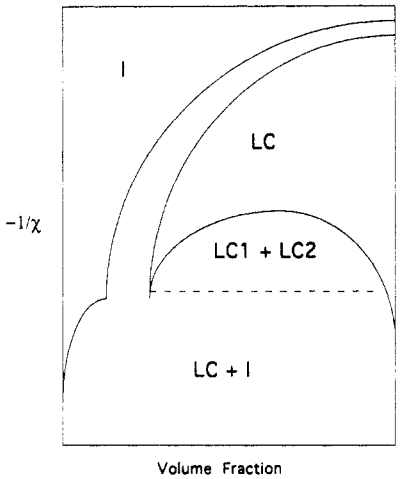

Figure 1. Schematic Flory phase diagram.

benzyl alcohol is particularly rich. At least six phases have been reported: an isotropic phase (I), two liquid crystalline phases (LC1 and LC2) which can coexist,[18,19] two types of crystallites (A and B),[20,21] and a thermoreversible gel phase.[22] Although the gel phase has been the subject of several previous studies, the techniques employed previously measured bulk properties which provide only indirect evidence about the nature of the gel phase on a molecular level and its relationship to the other phases. In the present study we obtain direct evidence about the nature of the gel phase on a molecular level by scrutinizing the vibrational spectra of PBLG/BA gels. The liquid crystalline aspects of the PBLG in several solvents have been investigated by several workers.[23-25] Miller and coworkers have mapped the phase diagram of PBLG in dimethylformamide (DMF)[24,26,27] and found good agreement with predictions of the Flory theory. In the Flory theory,[28] the free energy of the system is represented by entropic terms calculated from the polymer axial ratio and polymer volume fraction and a single interaction parameter χ, which is assumed to be small. No specific interactions involving the solvent are assumed. According to the Flory model, at low polymer concentrations and/or high temperatures a solution of polymer rods is isotropic. At high polymer concentrations or low temperatures the solution is liquid crystalline. For intermediate conditions the system is biphasic. A sketch of the Flory phase diagram is given in Figure 1. The Flory theory is expected to break down if attractive polymer–polymer interactions are of *magnitude greater than about* $0.2k_BT$. This may well happen in the biphasic region as a gel to sol transition apparently uncorrelated with the liquid crystal phases is observed in this region.[19] To explain gelation in addition to liquid crystallinity, the theory must be extended by including previously neglected terms. These neglected terms include specific polymer–polymer interactions, polymer–solvent interactions, and solvent ordering. The present study gives results pertaining to polymer–polymer and polymer–solvent interactions. A Raman study of the polymer–solvent interaction and a Raman study of ordering in benzyl alcohol alone are given in separate publications.[29,30]

Previous studies have shown that aggregates exist in PBLG/BA systems below about 65 °C regardless of whether the solution is isotropic or liquid crystalline.[19] The crystallinity of these aggregates as measured by X-ray diffraction improves going from concentrated liquid crystalline solutions to dilute isotropic solutions. Horton and Donald[19] attribute this variation in crystallinity to differences in polymer mobility. Sasaki et al.[20,21] identify two types of crystallite A and B which differ in melting point and polymer volume fraction. Type A crystallites are formed by slow cooling with gelation occurring between 48 and 60 °C. These workers identified type A crystals with the "complex phase" of volume fraction 0.76, which has been studied extensively in the PBLG/DMF system.[17,31-34] The complex phase is trigonal (a = 3.5 nm) with four polymer chains per asymmetric unit and one BA molecule for every two monomer units.[20] Parry and Elliott[17] proposed that the trigonal ordering is achieved by a quasi helical stacking of benzene rings. The B-type crystallites are formed by repeated quenching cycles and have a polymer volume fraction of 0.95. This phase may be considered to be a pure polymer phase which is swollen by a few solvent molecules.

The nature of each phase enumerated above is amenable to investigation by spectroscopic techniques. A review of spectroscopic investigations into the phase transitions of biopolymer systems is given by Bulkin.[35] The present study builds upon this earlier work. It is anticipated that a better understanding of the gelation process at the molecular level will provide the basis for extending existing theories to encompass the phenomenon of gelation.

Experimental Details

Infrared absorbance spectra were recorded with a Mattson 4020 FTIR spectrometer equipped with a DGTS detector. The spectrometer was well purged with dry nitrogen gas. CaF_2 transmission cells with spacers ranging from 9 to 23 μm were used. For most runs, 100 interferograms collected at 1-cm^{-1} resolution were co-added. For some runs 2-cm^{-1} resolution was used to eliminate the effects of channel fringes due to the 2-mm window thickness. Beer–Norton strong apodization was used in the Fourier transformation which reduced the effective resolution by a factor of 1.60.[36]

Samples of PBLG (MW 28 000, 85 000, and 345 000) were obtained from Sigma Chemical Co. Anhydrous grade BA (>99%) was obtained from Aldrich and stored under argon. The following gel preparation procedure was used. Approximate quantities of PBLG were transferred to preweighed 5-mL vials. These vials were then placed in a vacuum chamber to remove any adsorbed water and weighed to determine the quantitity of PBLG. An approximate volume of BA was added to the vials under an argon atmosphere. The vials were sealed with ground glass stoppers, removed from the glovebox, and weighed. The volume fraction of PBLG was calculated by assuming densities of 1.264 g/cm^3 for PBLG and 1.042 g/cm^3 for BA. Polymer and solvent were allowed to mix at 60 °C for not less than 2 weeks and then stored at room temperature.

Samples were heated to 65 °C and injected into sample cells preheated to the same temperature and then allowed to cool to room temperature. Room temperature spectra taken within an hour of injection resemble spectra of the same sample at temperatures above 65 °C. The spectral profile changes over several hours reach a limiting profile within 12 h. The gelation

Table II
Optical Characteristics of PBLG/BA Samples

molecular weight	vol fraction (%)	optical appearance
28 000	9.00	isotropic
85 000	8.85	birefringent
345 000	2.98	isotropic
345 000	9.06	birefringent
345 000	14.99	birefringent
345 000	20.94	birefringent
345 000	26.40	birefringent

kinetics are the subject of ongoing investigations, and the results will be reported in a future publication. No further changes in the amide bands were observed if the sample was aged for 4 days at room temperature, even though the visual appearance continued to evolve. A minimum of 12 h at room temperature was allowed for gel formation prior to each heating run. The annealing time was used to ensure a good nitrogen purge of the spectrometer. For a small number of samples, water vapor absorption peaks remained after purging. In the worst case, the water vapor peak at 1670 cm^{-1} had 2% of the amide I intensity at 1655 cm^{-1}. In these cases, water vapor was removed from the spectra by spectral subtraction.

The temperature dependence with monotonic heating of infrared spectra from six PBLG/BA samples was examined in detail. Four of these samples—volume fractions 3%, 9%, 15%, and 21%—were prepared with 345 000 MW PBLG to explore the effect of changing concentration. Results from a 26% sample of this molecular weight are not included because this sample showed signs of thermal decomposition. Two further samples—volume fraction 9% and PBLG molecular weights of 28 000 and 85 000—were examined together with the 9% 345 000 MW sample to look for any molecular weight dependence in the temperature-induced effects. For comparison, the temperature dependence of infrared spectra from pure BA and PBLG was also examined. The volume fraction, molecular weight, and optical characteristics under crossed polars of these samples are given in Table II. Two samples, $PBLG_{345000}$/BA 26% and $PBLG_{85000}$/BA 9%, were examined from 0 to 120 °C. Because most of the observed temperature dependence occurred between 30 and 80 °C, subsequent experiments were limited to the 30–80 °C range. The temperature dependence outside this range is well represented by linear extrapolation from the 30–80 °C range.

Curve Fitting. Several factors contribute to the observed absorbance at each point in the raw spectra. There is a background absorbance which includes terms arising from the frequency dependence of the refractive index and from scattering by fluctuations in the refractive index on a length scale comparable to the wavelengths of infrared radiation. Several workers have studied scattering by inhomogeneities with characteristic sizes of a few micrometers in PBLG solutions.[37-39] These contributions are of no interest in the present study and are approximated by a linear baseline. Absorption peaks in the raw spectra overlap. The relative contributions of each absorption to the observed profile can be estimated by a combination of deconvolution and curve fitting. The integrated area of each absorption peak depends upon the molecular concentration, the orientation of its transition dipole moment with respect to the incident radiation, and the magnitude of the dipole transition moment of the species undergoing a vibrational transition. The amide I band exhibits a large dichroic ratio of 2.9[6] so that orientational effects, which are not controlled in this study, could swamp the contributions due to other effects. Volchek et al.[40] have studied the temperature-dependent relaxation of an initial flow-induced orientation parallel to CaF_2 plates to a perpendicular orientation by monitoring the dichroic ratio. In the present study, the amide I spectra are deconvoluted prior to curve fitting to factor out orientation effects. In the deconvolution process peak frequency information is isolated, but peak shape information is lost. In the present investigation we focus on amide I peak frequencies.

Different procedures were followed for fitting peaks in the amide I and ester regions. For the amide I region (1620–1700 cm^{-1}), only the peak frequencies were of interest. Absorption spectra were deconvoluted in the 1520–1800-cm^{-1} range using an enhancement factor of $K = 2.2$ and by assuming a Lorentzian fwhm of 11.0 cm^{-1}. Details of the deconvolution process are given in the following section. The next stage of data reduction was fitting the deconvoluted spectra. Three models were tried. Each model contained a linear (slope plus intercept) background and two peaks with Gaussian, Lorentzian, or mixed Gauss–Lorentz character. The deconvoluted amide I peaks are resolved at 30 °C so that their deconvolved relative widths can be determined. It is assumed that the peak widths do not change very much with increasing temperature and that the parallel and perpendicular peaks change at roughly the same rate. Using these criteria, the most consistent results were obtained with the Gaussian model. The other models increased the width (and Lorentzian content) of the stronger parallel band and decreased the width (and Lorentzian content) of the weaker perpendicular band with increasing temperature. Results given in the next section are based on the Gaussian model. For each data set, the fit to the lowest temperature deconvoluted spectrum was refined first and used as the starting point for the next fit. In general, the starting parameters for fit n came from fit $n - 1$ with $T_{n-1} < T_n$. The deconvolution and peak fitting were carried out using the programs DECON and CURVEFIT, respectively, which are included in Mattson Advanced FIRST software.

The ester region (1685–1785 cm^{-1}) contains two broad bands near 1735 and 1715 cm^{-1} which arise from free and hydrogen-bonded ester groups, respectively. Each of these bands consists of several rotameric components which become partially resolved with deconvolution. The signal to noise ratio is degraded in the deconvolution process so that quantitative information about individual components of the weaker hydrogen-bonded ester band is lost. For this reason, the raw spectra rather than deconvoluted spectra were used for the peak fitting step for the ester region. The free and hydrogen-bonded ester band profiles were modeled as a sum of two Gaussian peaks plus a linear background. The most stable fits were obtained by taking the fit to the 55 °C spectrum as the starting point for all refinements. Integrated areas of the peaks were read into a separate, purpose-written program, and the H-bonded fraction was calculated as

$$X_H = \left(\frac{A_H}{rA_F + A_H}\right) \quad (1)$$

where A_F and A_H are the integrated areas of the free and hydrogen-bonded ester peaks near 1735 and 1715 cm^{-1}, respectively, and r is the ratio of absorption coefficients k_H/k_F. This ratio has been determined to range between 1.5 and 1.6 by other workers,[41-44] We adopt the value $r = 1.5$ for the present work. It must be stressed that the integrated areas of the peaks are strongly dependent upon the baseline taken. If deconvoluted spectra are fitted in the ester region, the hydrogen-bonded fraction is increased by a factor of approximately 3 at all temperatures. However, the shape of the H-bonded fraction vs temperature curve is the same (aside from a scaling factor) regardless of the choice of refinement conditions.

A lucid account of the deconvolution process is given by Cameron and Moffatt.[45] In the deconvolution process, unresolved peaks in a high signal to noise spectrum are exchanged for resolved peaks with the same integrated area at a lower signal to noise ratio. This is accomplished by making use of the detailed shape of the band profile. Deconvolution cannot enhance resolution beyond the measurement resolution. In the present study, spectra recorded at 4-cm^{-1} resolution or worse contained insufficient information to characterize the small shifts observed after deconvolution. The main factor limiting the degree of deconvolution possible in our spectra was imperfect cancellation of sharp water vapor absorptions. The effect of water vapor absorptions was minimized as described previously. For an enhancement factor of 2.2 the noise increases by just over 2 orders of magnitude and the fwhm of the peaks is decreased by a factor of about 2.2. The extent of deconvolution used was the minimum required to extract the amide I peak maxima over the whole temperature range rather than the maximum justified by the experimental S/N ratio. This conservation selection of deconvolution minimizes the risk of spurious features which appear in overdeconvoluted spectra. Our assumption of an intrinsic fwhm of 11.0 cm^{-1} was justified retroactively by fitting undeconvoluted amide I spectra. The peak centers were obtained from decon-

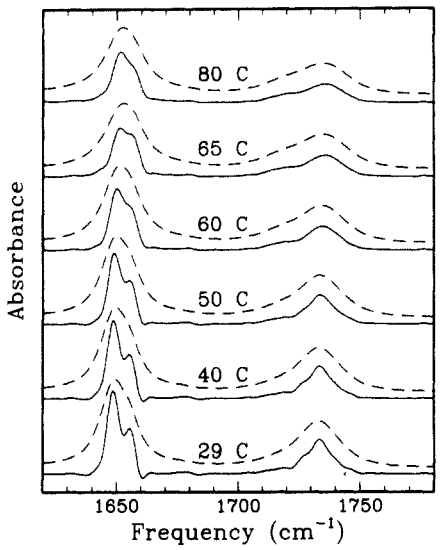

Figure 2. Normal (- - -) and deconvoluted (K = 2.2; W = 11.0 cm^{-1}) (—) infrared spectra of PBLG$_{345000}$/BA 15% at 29, 40, 50, 60, 65, and 80 °C in the amide I and ester region.

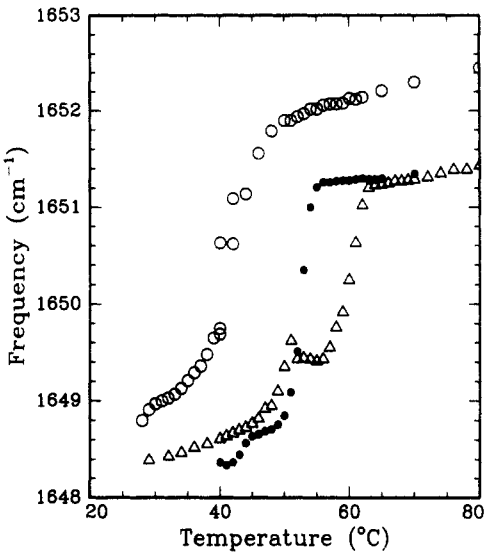

Figure 3. Temperature dependence of the amide I parallel band frequency for PBLG/BA samples of varying molecular weights: (○) MW = 28 000; (●) MW = 85 000; (◇) MW = 345 000.

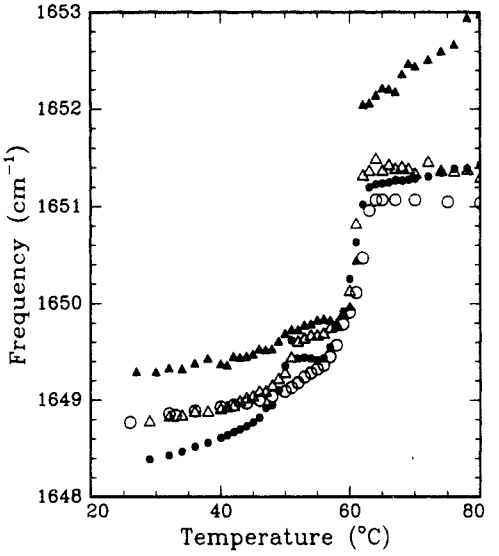

Figure 4. Temperature dependence of the amide I parallel band frequency for PBLG$_{345000}$/BA samples of varying concentrations: (○) 3%; (●) 9%; (△) 15%; (▲) 21%.

voluted spectra and held fixed for all but the last three cycles of refinement. The peak centers shifted by less than 0.02 cm^{-1}, and fwhm values of 12.7 and 16.3 cm^{-1} were obtained for the parallel and perpendicular components, respectively. If the assumed fwhm is too large, negative side lobes appear, whereas a smaller value merely limits the deconvolution achieved. In a previous study[12] an enhancement factor of K = 3.0 and a fwhm of 12.0 cm^{-1} were assumed.

Results

Infrared spectra from all PBLG/BA samples examined exhibit a similar temperature dependence in the 1620–1780-cm^{-1} region which contains the amide I bands near 1655 cm^{-1} and the ester bands near 1730 cm^{-1}. A typical temperature sequence (PBLG$_{345000}$/BA 15 v/v %) of raw and deconvolved infrared spectra is given in Figure 2. At room temperature the band profile is noticeably asymmetric with the parallel and perpendicular components partially resolved in the raw spectrum and fully resolved in the deconvoluted spectrum. The relative intensities of these components depend upon the orientation of PBLG molecules relative to the incident infrared radiation.

A transition is evident by inspection in the amide I region (1620–1700 cm^{-1}) between 60 and 65 °C for the 345 000 MW samples. The pattern is similar for lower molecular weight samples except that the transition occurs at a lower temperature. At temperatures below this critical temperature, T_c, the two components are fully resolved and easily fit as a sum of two Gaussian peaks with uncertainties in peak frequencies between 0.03 and 0.10 cm^{-1}. The spectra are mildly overdeconvoluted in the amide I region for $T < T_c$ as evidenced by the negative side lobes. The choice of deconvolution parameters was dictated by requirements for the $T > T_c$ region. In the transition temperature range ($T_c \pm 3$ °C), the peaks are not fully resolved and the fitting problem is ill-conditioned in some cases. The uncertainties generated by the fitting routines in this region are of order 0.2 cm^{-1}. For $T > 65$ °C, the peaks are again resolved. The uncertainties in peak frequencies are of order 0.15 cm^{-1}. The variation of amide I parallel peak frequencies determined by the fitting routine as a function of temperature for 9% solutions of 345 000, 85 000, and 28 000 MW PBLG is given in Figure 3, and the variation of amide I parallel peak frequencies as a function of temperature for four concentrations are given in Figure 4. The temperature dependence of the amide I perpendicular peak frequencies mirrors that of the parallel frequencies except that the magnitude of the shifts is smaller. Plots of the amide I perpendicular band frequencies are available on request.

Two transitions are evident in the PBLG$_{345000}$/BA 9% curve (Figure 3) near 52 and 62 °C. As the molecular weight is decreased, both transitions move to lower temperatures. As the concentration is decreased (Figure 4), the magnitude of the shift near 52 °C diminishes. The four concentrations have the same temperature dependence near the 62 °C transition. We can generalize the temperature dependence of all the samples between the lowest and highest temperatures sampled. The frequencies of the parallel and perpendicular bands at 30 °C are 1648 ± 0.2 and 1655.8 ± 0.4 cm^{-1}, respectively. The parallel frequency is significantly lower than the previously reported value[6] of 1652 cm^{-1}. This suggests that a further correction to the dichroic ratio of the amide I band given in Tsuboi's[6] classic work is required to account for the greater than anticipated contribution of the perpendicular peak to parallel peak absorbance. Above the highest transition temperature, the parallel and perpendicular frequencies become 1651.4 ± 0.4 and 1657.2 ± 0.4 cm^{-1},

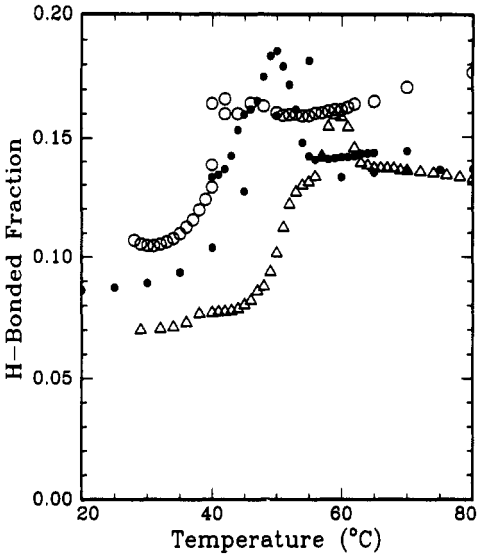

Figure 5. Temperature dependence of the hydrogen-bonded ester fraction for PBLG/BA 9% samples of varying molecular weights: (○) MW = 28 000; (●) MW = 85 000; (△) MW = 345 000.

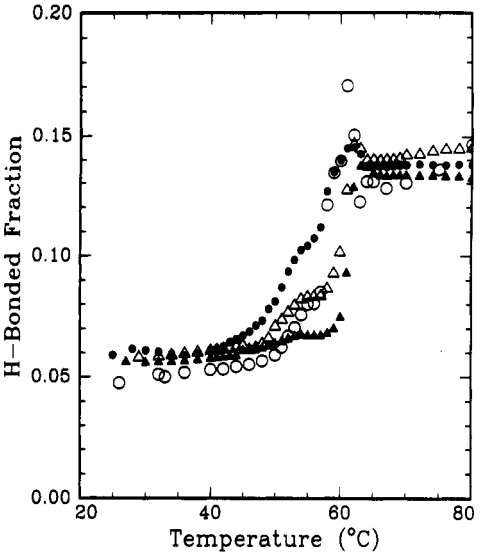

Figure 6. Temperature dependence of the hydrogen-bonded ester fraction for $PBLG_{345000}$/BA samples of varying concentrations: (○) 3%; (●) 9%; (△) 15%; (▲) 21%.

respectively. The frequency shifts are 2.6 and 1.4 cm^{-1}, respectively. The uncertainties in the shift are determined by the uncertainties in a single data set (rather than the scatter from all sets) to be about 0.3 cm^{-1}.

For the $PBLG_{345000}$/BA 26% sample, extra bands near 1668 and 1681 cm^{-1} appear and are probably indicative of decomposition. The extra peaks may be attributed to a combination of short helical segments and disordered regions. Nevskaya et al.[15] calculated the mode splittings for finite helical segments assuming transition dipole moment coupling interactions. These calculations suggest that helical segments with six or seven residues can account for the 1668-cm^{-1} band. In similar transition dipole moment coupling calculations, Painter and Coleman[46] modeled splittings between A and E modes for disordered regions based upon the assumption that the disordered structure resides in the same region of the Ramachandran plot as the parent ordered structure. The lowest frequency amide I peak is at 1648 cm^{-1}. This sets a lower frequency limit for the A mode of the disordered regions. Frequency shifts of between 5 and 20 cm^{-1} are predicted for the region of the Ramachandran plot containing the α-helix and presumably disordered structures derived from the α-helix. The extra peak at 1668 cm^{-1} is within the allowed range. The 1668-cm^{-1} peak displays a linear temperature dependence. The linear temperature dependence of the amide I random coil mode through the transition region demonstrates that the observed transitions are specific to sufficiently long segments of α-helical PBLG. The presence of disordered and short helical segments is expected to alter the phase diagram for this sample. Previous work by Volchek et al.[47] on a blend of α-helical PBLG and random coil polystyrene showed that random coil polystyrene mixes with the isotropic phase of PBLG but is rejected from the liquid crystalline phase of PBLG. We can infer that random coil regions of PBLG will also be rejected from liquid crystalline PBLG regions. This separation is expected on entropic grounds.

The temperature dependence of the hydrogen-bonded ester fraction calculated from eq 1 as functions of molecular weight and concentration are given in Figures 5 and 6, respectively. The peak widths and frequencies of both components change in a similar manner to the bonding fraction. For all runs, the H-bonded fraction is ca. 0.06 below 50 °C and ca. 0.14 above 65 °C. Two transitions

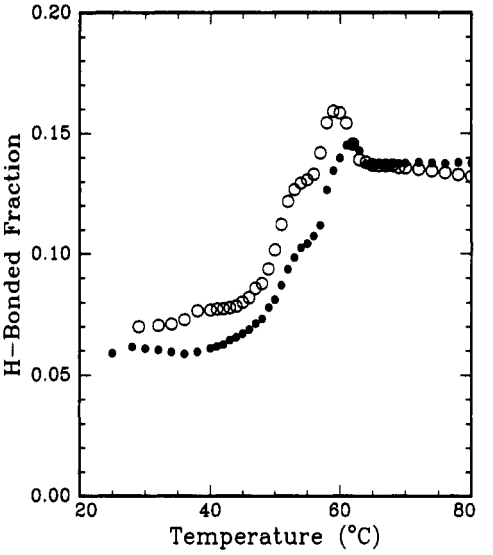

Figure 7. Temperature dependence of the hydrogen-bonded ester fraction for $PBLG_{345000}$/BA 9% samples: (○) injected 65 °C; (●) injected 75 °C.

near 52 and 62 °C are observed for all runs. The magnitude of the change at 52 °C is dependent upon the thermal history of the sample. This is illustrated in Figure 7 for a 9% sample of $PBLG_{345000}$ which was subject to different thermal treatments. For the first run, the sample was injected at 65 °C and cooled to room temperature. For the second run, the sample was injected and annealed at 75 °C for 30 min prior to cooling to room temperature. Both samples were held at room temperature for 12 h prior to the heating run. The heat treatment reduces the H-bonded fraction for all $T < 62$ °C. The temperature dependence of the amide I, ester H-bonded fraction, and DSC traces is similar. For comparison purposes, the DSC trace for the $PBLG_{345000}$/BA 9% sample is superimposed over the temperature dependence of the amide I parallel and H-bonded ester fraction plots in Figure 8.

Discussion

The agreement between transition temperatures obtained by infrared, DSC, and modulus[22] measurements is striking. The positioning of these transition temperatures, however, involves a degree of subjective judgment and

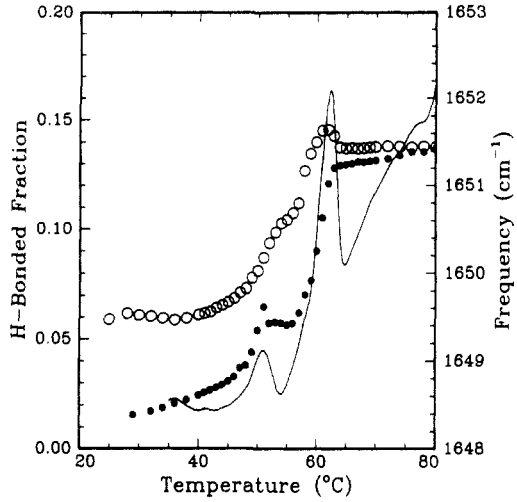

Figure 8. Temperature dependence of DSC trace (—), hydrogen-bonded ester fraction (○), and amide I parallel band frequency (●) for $PBLG_{345000}$/BA 9% samples.

results in a loss of information. A better comparison between results from different techniques is obtained by comparing the shapes of the temperature-dependent curves.

Comparisons between techniques are most readily made for $PBLG_{345000}$/BA 9% samples due to the availability of data from infrared, DSC, modulus, and light scattering. A small increase in the fraction of hydrogen-bound ester occurs near 38 °C (Figure 8). We call this transition I. Fukuzawa et al.[48] observed a change in the modulus of a PBLG film at 38 °C and assigned it to the onset of side-chain motions. It is reasonable to expect solvent penetration of the side chains to increase with side-chain melting so that we adopt this mechanism as the most probable cause of transition I. The sharp increase in the fraction of hydrogen-bound ester groups near 52 °C, which we dub transition II, corresponds closely to the decrease in the rigidity modulus in the same temperature range reported by Hill and Donald.[22] We believe that the H-bonding is between BA and PBLG and interpret the increased H-bonding as being due to an increased polymer surface area exposed to solvent. A DSC endotherm occurs at this temperature which must correspond to the hydrogen-bonding energy. The amide I parallel peak exhibits a concentration-dependent shift of approximately 0.3 cm^{-1} to higher frequency in transition II. This transition is also manifest as a decrease in the quadrupolar splitting and line width of deuterium NMR peaks in a similar system.[49] The NMR transition temperature is in broad agreement with the present results if the difference in sample molecular weight is taken into account. A third transition, III, occurs at 62 °C for this sample. The behavior of the hydrogen-bonded ester fraction suggests that this is a two-stage process. The hydrogen-bound fraction increases with temperature from less than 0.10 to ca. 0.15 at the midpoint of the transition. As the temperature is increased further, the fraction falls to a plateau value of ca. 0.14. We interpret this as a solvent-catalyzed transition. In the same temperature range, the remaining gel modulus is lost and the main DSC endotherm appears. The amide I peaks shift approximately 2 cm^{-1} to higher frequency at this temperature. The close correspondence between transition temperatures obtained by infrared, DSC, and modulus measurements demonstrates that different techniques are monitoring different aspects of the same transitions. We are therefore justified in treating the techniques as complementary to interpret the results.

Table III
Amide I Frequencies of Aggregated and Dispersed $PBLG_{85000}$

solvent	vol fraction (%)	T (°C)	sample condition	∥ band freq (cm^{-1})	⊥ band freq (cm^{-1})
benzyl alcohol	8.85	40	gel	1648.4	1655.5
benzyl alcohol	8.85	65	sol	1651.3	1657.8
methylene chloride	0.08	30	molecular dispersion	1651.8	1657.9

We now undertake the task of relating the observed spectroscopic changes to underlying molecular processes. We first discuss the nature of aggregation implied by the spectroscopic results and then proceed to discuss the mechanisms by which changes in aggregation may alter the spectra.

Nature of Aggregation. In the present study we rely upon previous work[18-22] to conclude that aggregates are present in our samples at appropriate temperatures. We now identify the presence of aggregates with specific spectroscopic features. To make this identification, spectra at the same temperature of samples known to be aggregated and molecularly dispersed are required. This is achieved by comparing spectra from a high concentration of PBLG in a poor solvent (BA) to spectra from a very dilute (0.08%) solution of PBLG in a good solvent (methylene chloride). Amide I frequencies for these limiting cases are summarized in Table III. The frequencies for the aggregated system (i.e., below the gel melting point) are lower by about 2 cm^{-1}. If the aggregated system is heated above the gel melting point, the amide I frequencies shift to the values observed for the dispersed system. From this we infer that PBLG in BA is also molecularly disperse above the gel melting temperature and attribute the shift to lower frequency with diminishing temperature to aggregation. Further evidence for this conclusion comes from the temperature dependence of spectra on cooling. As noted above, several hours are required for a sample to exhibit spectra characteristic of the gel state at room temperature following heating to above 65 °C. The time constant for this relaxation process is incompatible with a molecular relaxation process for which a time constant of milliseconds would be typical. The relaxation process observed must therefore be related to reorganization on a supramolecular rather than a molecular scale.

The molecular weight dependence of the amide I and ester peaks (Figures 3 and 5) demonstrates that the interaction between polymer chains scales with the length. The aggregation in this case is clearly side by side rather than end to end, for which no molecular weight dependence is expected.

The gel melting process occurs in three stages as noted above. Transition I is assigned to the onset of side-chain motions in agreement with previous work. Transition III clearly corresponds to disaggregation of polymer bundles into individual polymer chains. The spectra taken at temperatures near transition III consist of a superposition of spectra from aggregated and disaggregated polymer. The origins of transition II remain uncertain. Below, we examine three hypotheses about the origins of transition II. First, transition II may correspond to the melting point of one population of aggregates. A second possibility is that transition II is a conformational change with no change in the state of aggregation. The third possibility is that transition II is part of a two-step process in which large fibrils break up into elementary fibrils during transition II and the elementary fibrils break up in transition III.

If transition II is the melting point of one crystal population into single chains, then the spectra at temperatures above transition II will be a superposition of peaks arising from aggregated and disaggregated polymer. Although additional peaks are not resolved, the amide I spectra can be fit over the entire temperature range by varying only the relative amplitudes of characteristic aggregated and disaggregated spectra. This is a possible rather than a unique interpretation. It is also possible to interpret transition II as a change in the relative concentrations of different types of aggregate with different characteristic frequencies. This is the preferred interpretation because spectra recorded at temperatures below transition III do not change if the heating rate is reduced to zero for several hours. This observation is consistent with polymer immobilized in subaggregates. The presence of a gel modulus between transitions II and III indicates the presence of aggregates which would, with time, nucleate the reaggregation of any free polymer. The kinetics of aggregation in the PBLG/BA system is the subject of ongoing experiments, the results of which will be given in a future paper.

If the second hypothesis were correct, then only minor changes in the modulus would be expected, contrary to observation. Furthermore, a shift in the amide I frequency during transition II is observed only for concentrated samples, which suggests a sensitivity to the liquid crystalline state following the transition rather than a conformational change during the transition. The large observed change in modulus during transition II is consistent with a disaggregation process rather than a conformational change.

A combination of the first and third hypotheses provides the best description of the present results. The third hypothesis fails to explain the visual observation of crystal melting[19] during transition III. The transition we observe must therefore correspond to incomplete disaggregation of only one type of aggregate in accordance with hypothesis 1. In this picture, the gel modulus is derived primarily from fibrils which melt into elementary fibrils during transition II. The remaining modulus is derived from connections between crystals which melt during transition III. We presume that the crystals melt at nearly the same temperature as the elementary aggregates. The assumed small difference in melting points of crystals and elementary aggregates would not be resolved if the crystals constitute only a small fraction of the polymer.

Our inference that the melting points of the crystals and the elementary fibrils is similar is unlikely to be coincidental. The elementary fibrils are likely to be structurally similar to the crystals. If the crystals belong to the "complex phase" shown to exist in the PBLG/BA system by Sasaki et al.,[20] then the elementary fibrils consist of a single asymmetric unit containing four polymer chains of the complex phase.

Several previous studies give an indication of the probable size of elementary fibrils. Volchek et al.[50] studied the phase diagram of PBLG in several solvents and calculated the effective asymmetry, which was slightly smaller than that expected for individual polymer rods, from Flory's theory. Differences between theory and experiment were reduced by addition of the disaggregating agent trifluoroacetic acid, implying the presence of small molecular clusters. These authors[14] attribute the disaggregating action of the acid to its screening effect on dipole–dipole interactions.

Iizuka[51] reviews results obtained from PBLG systems oriented by electric and magnetic fields. His results were interpreted in terms of molecular clusters possessing giant dipoles equivalent to 730 helices. On the basis of light scattering studies, he assumed that clusters are composed of nearly equal numbers of parallel and antiparallel helices. The giant dipole is presumed to arise from random fluctuations in the number of parallel dipoles in a cluster containing 5×10^5 helices. This size estimate corresponds to a cube of pure PBLG of dimension 0.5 μm and seems unrealistically large to us.

Intermolecular Interactions. There are three main mechanisms by which the magnitude of the amide I shifts at transition III might be explained. The first model supposes that the amide I mode is subject to an external perturbation arising from the mean dipole field generated by adjacent molecules. The second model assumes that a conformational change is the cause of the frequency shift. The third model takes group theoretical considerations into account. All of these models are speculative and subject to future experimental confirmation or rejection.

(1) Intermolecular Dipole Moment Model. The electric field generated by the permanent dipoles of a PBLG macromolecule can be decomposed into static and fluctuating terms. We consider the effects of fluctuating dipoles first and then proceed to the static case.

Phase relationships between fluctuating dipoles of the amide group give rise to the observed splitting between parallel and perpendicular components of the amide I band. With aggregation, the fluctuating dipoles of different helices are expected to be separated by approximately the diameter of a PBLG helix: 1.52 nm. If the model α-helix of Nevskaya and Chirgadze[15] is placed on a C_6 site of the space group $P6$ (a = 1.52 nm; c = 2.7 nm), the resonance frequencies are shifted by $\Delta\nu_A = 4.6$ cm^{-1} and $\Delta\nu_E = -0.3$ cm^{-1}. This model neglects the disorder inherent in the system and possible screening effects of the oppositely directed ester dipole moments. These effects are expected to diminish the magnitude of the predicted shift. Thus, the transition dipole model outlined above predicts frequency shifts similar in magnitude to those observed on aggregation. However, this model predicts that the A mode will shift to higher frequency, in stark contradiction to the observed shift to lower frequency. We conclude that transition dipole moment coupling between helices does not contribute significantly to the observed effects.

The electric field experienced by the amide helix core due to static molecular dipoles varies with the state of aggregation. This variation is caused by chemical changes and changes in geometrical factors. The net dipole moment of PBLG consists of opposing core and side-chain contributions.[52] Milstein and Charney[53] found that PBLG with hydrogen-bonded ester groups has a smaller net dipole moment than PBLG with unbound ester groups. Consequently, we expect the electric field to decrease coincident with an increase in the level of hydrogen bonding during transition II.

PBLG aggregates side by side in BA so that we can assume that the polymer chains are all either parallel or antiparallel within an aggregate. Because the amide I shift with aggregation is in the same direction as the shift due to hydrogen bonding within the helix, it is reasonable to assume that the polymer rods in a fibril are parallel. In the sol state a cholesteric liquid crystalline phase is formed so that we can assume that over a sufficiently small region nematic order prevails. For simplicity we assume perfect nematic order so that the polymer rods are all parallel or antiparallel. The static dipole moment associated with each polymer rod is equivalent to a charge separation.

Consider two planes separated by a distance d which are perpendicular to the polymer axis. Each area in such a plane will have a local charge density σ which is proportional to the number of polymer rods intersecting the plane per unit area weighted by the charge per rod. The other plane will have a local charge density $-\sigma$. The electric field generated between the planes will be

$$E = \sigma/\epsilon \quad (2)$$

In the disaggregated state the charge density will be uniform because there is no translational order perpendicular to the rod axes. The aggregated state will exhibit local charge concentrations surrounded by uncharged regions. In this case, the electric field experienced by an amide group in an aggregate will be larger than the electric field experienced by an amide group in the sol state. This geometrical factor, unlike the chemical factor, is concentration dependent.

We now outline the relationship between frequency shifts and the variation of the electric field noted above. It is well-known that the hydrogen bonds of an α-helix are anharmonic.[54] It is reasonable to assume that hydrogen bond anharmonicity contributes to anharmonicity in the amide I vibrational modes. In this case, the interaction between the amide I dipole transition moment and an electric field is expected to decrease the transition energies by an amount proportional to $\mathbf{E}\cdot\mu$.[55] The predicted ratio of parallel to perpendicular frequency shifts is cot θ. Tsuboi[6] gives the angle between the amide I transition dipole moment μ and the PBLG rod axis as 39° for PBLG film. Somewhat lower values of 35° and 34° are given by Iizuka[56] and Volchek et al.,[40] respectively, for PBLG for dichloromethane solution. Using these values for θ, we predict frequency shift ratios ranging from 1.235 to 1.482. The observed ratios for 28 000, 85 000, and 345 000 MW samples are 1.23, 1.43, and 1.73, respectively. This model thus explains the link between the H-bonded ester fraction and amide I frequency shifts but fails, however, to fully explain either the magnitude of the shifts or the dependence of the shifts upon overall polymer concentration.

(2) Conformational Change. Previous studies have shown that the conformation of helical PBLG can be distorted by constructing copolymers of PBLG with its enantiomorph PBDG. PBLG/PBDG copolymers and racemic mixtures of PBLG and PBDG have been thoroughly investigated by infrared[57,58] and Raman spectroscopy,[59] and NMR,[60] and X-ray diffraction.[61,62] The Raman study by Wilser and Fitchen[59] finds a shift in the amide I parallel (A) band of 1.4 cm^{-1} for a 50% copolymer of PBLG with PBDG. The helical pitch of this copolymer is 3.58 compared with 3.60 for pure PBLG. Changes in the helical pitch are attributed to changes in side-chain packing. The shift observed in the Raman study[59] is comparable in magnitude and direction to the amide I shifts observed in the present study so that it is reasonable to hypothesize that the helical pitch for aggregated PBLG is less than the helical pitch for disaggregated PBLG. Experiments are now underway to explore this possibility and will be communicated in a future publication.

(3) Group Theory. Up till now, our analysis of the amide bands has been based on the assumption that the 18/5 helix is of infinite extent and isolated from other helices. One unit cell of the helical "crystal" consists of 18 monomer units and has mass 3946 amu. The 28 000 MW sample with only 7 unit cells can hardly be approximated as infinite in extent. For this case, each vibration of the 7 unit cell chain splits into 7 components arising from vibrations between unit cells, all of which are optically active. The lowest frequency mode of each multiplet (corresponding to the largest phase difference between adjacent unit cells) is expected to shift to lower frequency and increase in relative intensity as the number of unit cells increases. Absorption peaks from a finite chain are thus expected to be assymetrically skewed to higher frequency.[63] The transition dipole moment coupling calculations of Nevskaya and Chirgadze[15] predict a band profile similar to an infinite helix but displaced to a slightly higher frequency. The amide I frequencies for the 28 000 MW sample are approximately 0.8 cm^{-1} higher than the amide I frequencies of the 345 000 MW samples at all temperatures measured. We note that aggregation is not expected to increase the effective chain length because the aggregation is side by side. Conversely, defects (possibly thermally induced) will have the effect of reducing a long chain into several shorter segments and increasing the frequency. In this model, the lowest peak frequency in the amide I band is expected to decrease with increasing molecular weight to a limiting value determined by the persistence length. Part of the frequency shifts noted in the present study may arise from thermally activated defects in the polymer chain.

We have insufficient evidence at present to test this hypothesis. If this hypothesis is correct, then the amide I band for low MW molecules consists of several closely spaced peaks with intensity increasing toward lower frequency. This would be manifest as a skewed peak shape if the spectral resolution could be improved sufficiently.

Conclusions. Aggregation in PBLG/benzyl alcohol systems has been studied by infrared spectroscopy. The amide and ester band frequencies are found to be sensitive indicators of the state of aggregation and provide the basis for future investigations of aggregation kinetics. PBLG/BA gels consist of side by side aggregates of PBLG which melt in three stages. Side-chain motions commence near 40 °C (I) and are followed by fragmentation of polymer bundles into elementary fibrils (II) and dissociation of these elementary fibrils into individual polymer chains (III). Transition temperatures for stages II and III are dependent upon molecular weight. Transition III may be accompanied by subtle conformational changes in the α-helical molecular structure which have not been observed previously by spectroscopic means. The present study demonstrates the potential of spectroscopic techniques to unravel another layer of complexity in protein and polypeptide systems.

Acknowledgment. This work was supported by funds provided by the AFRC. We are grateful to Prof. Ed Morris for helpful discussions.

References and Notes

(1) Ambrose, E. J.; Elliott, A. *Proc. R. Soc. London* **1951**, *A205*, 47.
(2) Perutz, M. F. *Nature* **1951**, *167*, 1053.
(3) Pauling, L.; Corey, R. B. *Proc. Natl. Acad. Sci. U.S.A.* **1951**, *37*, 241.
(4) Blout, E. R.; Asadourian, A. *J. Am. Chem. Soc.* **1956**, *78*, 955.
(5) Bradbury, E. M.; Brown, L.; Downie, A. R.; Elliott, A.; Fraser, R. D. B.; Hanby, W. E.; McDonald, T. R. R. *J. Mol. Biol.* **1960**, *2*, 276.
(6) Tsuboi, M. *J. Polym. Sci.* **1962**, *59*, 139.
(7) Masuda, Y.; Miyazawa, T. *Makromol. Chem.* **1967**, *103*, 261.
(8) Simons, L.; Bergstrom, G.; Blomfelt, G.; Forss, S.; Stenback, H.; Wansen, G. *Commenat. Phys.-Math.* **1972**, *42*, 125.
(9) Koenig, J. L.; Sutton, P. L. *Biopolymers* **1971**, *10*, 89.
(10) Chen, M. C.; Lord, R. C. *J. Am. Chem. Soc.* **1974**, *96*, 4750.
(11) Wilser, W. T.; Fitchen, D. B. *J. Chem. Phys.* **1975**, *62*, 720.
(12) Lipp, E. D.; Nafie, L. A. *Biopolymers* **1985**, *24*, 799.
(13) Renthal, R.; Taboada, J. *Phys. Lett. A* **1989**, *139*, 57.
(14) Krimm, S.; Abe, Y. *Proc. Natl. Acad. Sci. U.S.A.* **1972**, *69*, 2788.
(15) Nevskaya, N. A.; Chirgadze, Yu. N. *Biopolymers* **1976**, *15*, 637.

(16) Fanconi, B.; Tomlinson, B.; Nafie, L.; Small, W.; Peticolas, W. *J. Chem. Phys.* **1969**, *51*, 3993.
(17) Parry, D. A. D.; Elliott, A. J. *J. Mol. Biol.* **1964**, *25*, 1.
(18) Hill, A.; Donald, A. M. *Mol. Cryst. Liq. Cryst.* **1987**, *153*, 395.
(19) Horton, J. C.; Donald, A. M. *Polymer* **1991**, *32*, 2418.
(20) Sasaki, S.; Hikata, M.; Shiraki, C.; Uematsu, I. *Polym. J.* **1982**, *14*, 205.
(21) Sasaki, S.; Tokuma, K.; Uematsu, I. *Polym. Bull.* **1983**, *10*, 539.
(22) Hill, A.; Donald, A. M. *Polymer* **1988**, *29*, 1426.
(23) Robinson, C.; Ward, J. C.; Beevers, R. B. *Discuss. Faraday Soc.* **1958**, *25*, 29.
(24) Wee, E. L.; Miller, W. G. *J. Chem. Phys.* **1971**, *75*, 1446.
(25) Ginzberg, B.; Siromyatnikova, T.; Frenkel, S. *Polym. Bull.* **1985**, *13*, 139.
(26) Rai, J. H.; Miller, W. G. *J. Phys. Chem.* **1972**, *76*, 1081.
(27) Miller, W. G.; Kou, L.; Tohyama, K.; Voltaggio, V. *J. Polym. Sci., Polym. Symp.* **1978**, *65*, 91.
(28) Flory, P. J. *Proc. R. Soc. London A* **1956**, *234*, 73.
(29) Prystupa, D. A.; Torrie, B. H. Unpublished results.
(30) Prystupa, D. A. Unpublished results.
(31) Luzzati, V.; Cesari, M.; Spach, G.; Mason, F.; Vincent, J. M. *J. Mol. Biol.* **1961**, *3*, 566.
(32) Sasaki, S.; Hikata, M.; Shiraki, C.; Uematsu, I. *Rep. Prog. Polym. Phys. Jpn.* **1978**, *21*, 557.
(33) Watanabe, J.; Kishida, H.; Uematsu, I. *Polym. Prepr. Jpn.* **1981**, *30*, 279.
(34) Russo, P. S.; Miller, W. G. *Macromolecules* **1984**, *17*, 1324.
(35) *Infrared and Raman Spectroscopy of Liquid Crystals*; Bulkin, B. J., Ed.; Dekker: New York, 1979; pp 365–410.
(36) Norton, R. H.; Beer, R. J. *Opt. Soc. Am.* **1976**, *66*, 259.
(37) Shulka, P.; Muthukumar, M. *J. Polym. Sci. B: Polym. Phys.* **1991**, *29*, 1373.
(38) Shulka, P.; Muthukumar, M.; Langley, K. H. *J. Appl. Polym. Sci.* **1992**, *44*, 2115.
(39) Russo, P. S.; Magestro, P.; Miller, W. G. *ACS Symp. Ser.* **1987**, *No. 350*, 152.
(40) Volchek, B. Z.; Gribanov, A. V.; Kol'sov, A. I.; Purkina, A. V.; Vlasov, G. P.; Ovsyannikova, L. A. *Vysokomol. Soedin.* **1977**, *A19*, 519.
(41) Bhagwagar, D. E.; Painter, P. C.; Coleman, M. M. *Macromolecules* **1992**, *25*, 1361.
(42) Coleman, M. M.; Graf, J. F.; Painter, P. C. *Specific Interactions and the Miscibility of Polymer Blends*; Technomic Publishing: Lancaster, PA, 1991.
(43) Moskala, E. J.; Howe, S. E.; Painter, P. C.; Coleman, M. M. *Macromolecules* **1984**, *17*, 1671.
(44) Coleman, M. M.; Lichkus, A. M.; Painter, P. C. *Macromolecules* **1989**, *22*, 586.
(45) Cameron, D. G.; Moffatt, D. J. *J. Test. Eval.* **1984**, *12*, 78.
(46) Painter, P. C.; Coleman, M. M. *Biopolymers* **1978**, *17*, 2475.
(47) Volchek, B. Z.; Purkina, A. V.; Merkur'yeva, A. A.; Vlasov, G. P.; Ovsyannikova, L. A.; *Vysokomol. Soedin.* **1984**, *A26*, 711.
(48) Fukuzawa, T.; Uematsu, I.; Uematsu, Y. *Polym. J.* **1974**, *6*, 431.
(49) Poliks, M. D.; Park, Y. W.; Samulski, E. T. *Mol. Cryst. Liq. Cryst.* **1987**, *153*, 321.
(50) Volchek, B. Z.; Purkina, A. V.; Vlasov, G. P.; Ovsyannikova, L. A. *Mol. Cryst. Liq. Cryst.* **1981**, *73*, 283.
(51) Iizuka, E. *J. Appl. Polym. Sci.: Appl. Polym. Symp.* **1985**, *41*, 131.
(52) Wada, A. In *Poly-a-Amino Acids: Protein Models for Conformational Studies*; Fasman, G. D., Ed.; Dekker: New York, 1967; Vol. 1, pp 369–390.
(53) Milstein, J. B.; Charney, E. *Biopolymers* **1970**, *9*, 991.
(54) Scott, A. C. *Phys. Rev. A* **1982**, *26*, 578.
(55) Coggeshall, N. D. *J. Chem. Phys.* **1950**, *18*, 978.
(56) Iizuka, E. *Polym. J.* **1975**, *7*, 650.
(57) Tsuboi, M.; Wada, A.; Nagashima, N. *J. Mol. Biol.* **1961**, *3*, 705.
(58) Tsuboi, M.; Mitsui, Y.; Wada, A.; Miyazawa, T.; Nagashima, N. *Biopolymers* **1963**, *1*, 297.
(59) Wilser, W. T.; Fitchen, D. B. *Biopolymers* **1974**, *13*, 1435.
(60) Watanabe, J.; Imai, K.; Kosaka, K.; Abe, A.; Uematsu, I. *Polym. J.* **1981**, *13*, 603.
(61) Mitsui, Y.; Iitaka, Y.; Tsuboi, M. *J. Mol. Biol.* **1967**, *24*, 15.
(62) Squire, J. M.; Elliott, A. *J. Mol. Biol.* **1972**, *65*, 291.
(63) Painter, P. C.; Coleman, M. M.; Koenig, J. L. *The Theory of Vibrational Spectroscopy and its Application to Polymeric Materials*; Wiley: New York, 1990; p 353.